Geologie en Mijnbouw **73:** 199–214, 1994.

Fault-plane solutions and source parameters of the 1992 Roermond, the Netherlands, mainshock and its stronger aftershocks from regional seismic data

Ludwig Ahorner
Department of Earthquake Geology, Geological Institute, University of Cologne, Vinzenz-Pallotti-Str. 26, D-51429 Bergisch Gladbach, Germany

Received 14 June 1993; accepted in revised form 10 November 1993

Key words: Roermond earthquake, Peel Boundary Fault, Roer Valley Graben, Lower Rhine Embayment

Abstract

The earthquake of April 13, 1992 in the border region between the Netherlands and Germany near the town of Roermond, ranges with its local magnitude of M_L = 5.9 among the largest seismic events observed in historical times in the Lower Rhine Embayment. Several hundred buildings in the area around the epicenter suffered light to moderate structural damage (intensity VII effects). The mainshock was preceded about 0.2 seconds before by a foreshock of local magnitude $M_L \approx 4.8$ and followed, up to the middle of May, by more than 200 aftershocks with local magnitudes up to M_L = 3.8.

The whole earthquake sequence has been well recorded by the dense seismic station network in the Lower Rhine Embayment and its vicinity. Based on these local and regional recordings the hypocenter locations, source parameters and focal mechanisms of the stronger events of the sequence have been determined with high precision by the Department of Earthquake Geology of the University of Cologne.

The source of the mainshock was located in the southwestern vicinity of Roermond, about 14 to 18 km below the surface at the depth continuation of the Peel Boundary Fault. This fault zone forms the eastern border of the Roer Valley Graben. The focal mechanism was of the extensional dip-slip type (normal fault) with the active fault plane trending in NW-SE direction (124°) and dipping steeply (at 68° to the SW). The western block (Roer Valley Graben) moved down with respect to the eastern block (Peel Horst). A diameter of the source area of 4 to 5 km has been determined from the spectral analysis of P- and SH-wave signals, using the Brune source model. The average displacement along the fault plane was approximately 21 cm, the associated static stress drop 4.4 MPa and the seismic moment 10^{17} Nm. The spatial distribution of the aftershocks points to a source zone which trends in the same general direction as the Peel Boundary Fault and has a total length of about 10 km. The main conclusions about the Roermond earthquake sequence fit well into the tectonic setting of the Lower Rhine Embayment and the general pattern of seismotectonic dislocations in the western and central European area.

Introduction

The Roermond earthquake of April 13, 1992 (Fig. 1), ranges with its local magnitude of M_L = 5.9 among the largest seismic events which have been observed in historical time in western Europe and especially in the Lower Rhine Embayment (Ahorner 1983, 1992, 1993; Houtgast 1992; Meidow & Ahorner 1994). Former strong earthquakes in this embayment during the last two centuries are the damaging earthquakes of Düren 1755 ($M_L \approx 5.8$), Düren 1756 ($M_L \approx 6.1$), Tollhausen 1878 ($M_L \approx 5.9$), Uden 1932 (M_L = 5.5) and Euskirchen 1951 (M_L = 5.7). The Uden (the Netherlands) earthquake was centered in the northwestern part of the Roer Valley Graben, outside the map area of Fig. 1, in a geological position quite similar to that of the 1992 Roermond earthquake.

The Roermond earthquake was felt in wide parts of central and western Europe over an area of approximately 600 000 km^2 (Haak et al. 1994; Meidow &

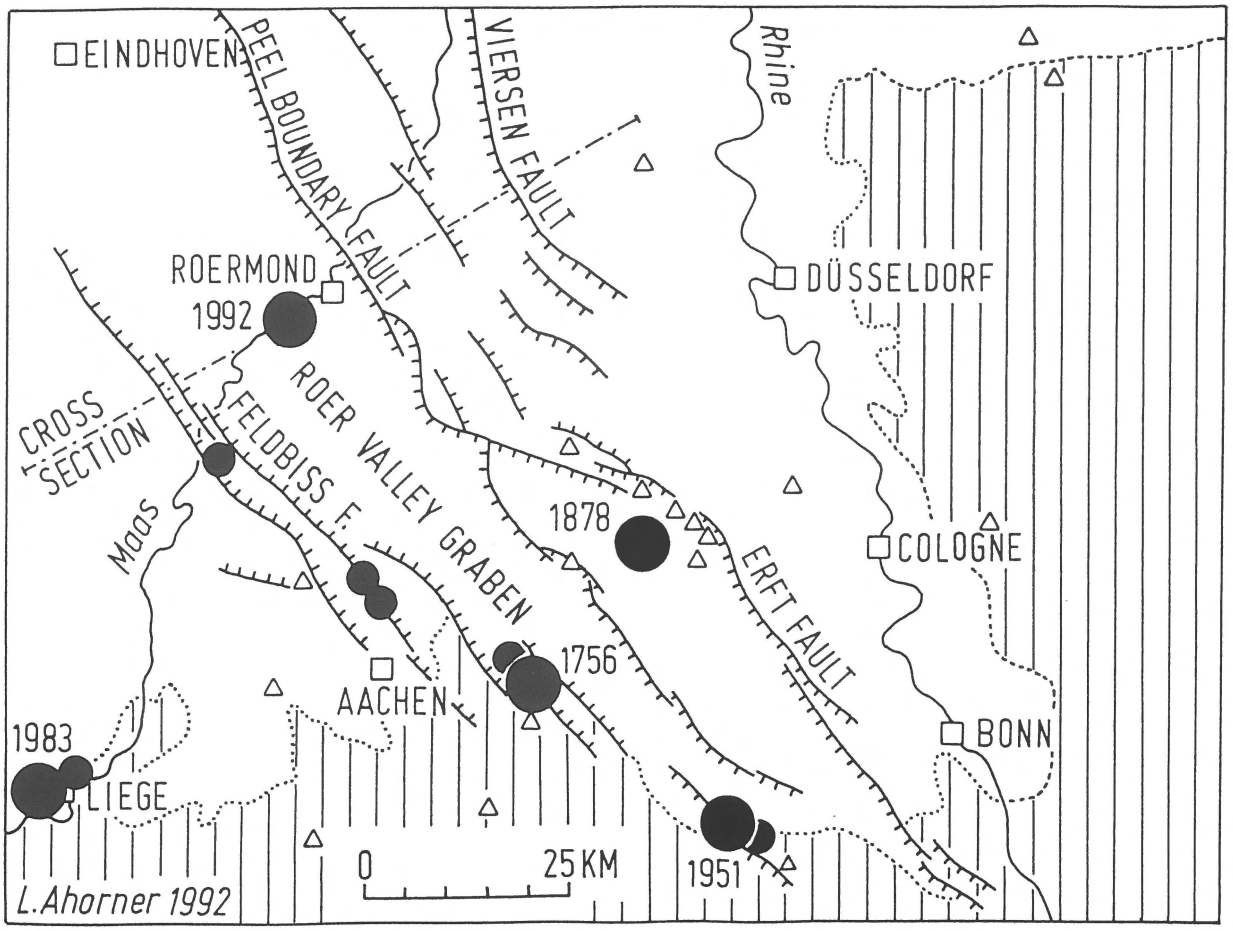

Fig. 1. Sketch map of the Lower Rhine Embayment with the epicenters of damaging earthquakes (filled circles) since 1750. For larger events with local magnitudes $M_L > 5.0$ (big circles) the year of occurrence is denoted. Active normal faults are drawn with barbs on the downthrown side (after Ahorner 1962). Permanent seismic stations are displayed by triangles. The cross-section is shown in Fig. 4.

Ahorner 1994). The most distant macroseismic reports came from Berlin, Munich, Zürich and southeast-England, more than 500 km from the epicenter. Several hundred buildings in the Netherlands-German border region around the epicenter suffered light to moderate structural damage (intensity VII effects). On German territory, slight damage was also reported from Aachen, Cologne, Euskirchen, Bonn and even from Koblenz, at an epicentral distance of 145 km. More than 40 persons were injured by the earthquake in Germany and in the Netherlands, mostly by falling debris. One women died from a heart attack at Bonn, Germany.

The mainshock and its stronger aftershocks have been well recorded by the dense seismic station network of the Lower Rhine Embayment and in the adjoining Rhenish Massif. Consequently, the hypocenter coordinates, fault-plane solutions and source parameters of the Roermond earthquake sequence can be determined with high precision using local and regional seismic data.

This paper describes the results of a comprehensive study of the Roermond earthquake sequence carried out at the Department of Earthquake Geology of the Geological Institute of the University of Cologne. The study is based mainly on high-quality digital seismogram recordings obtained in the distance range of up to about 150 km from the source area.

Station networks

The records of more than 30 permanent seismic stations, which were operating in the Lower Rhine

Embayment and the neighbouring Rhenish Massif within 100 km from the epicenter, are of special importance for a detailed source analysis of the Roermond earthquake sequence. These permanent stations belong to local seismic networks of the universities of Cologne and Bochum, the Geological Survey of North-Rhine-Westfalia (GLA), the Royal Belgian Observatory (ORB) and the Royal Netherlands Meteorological Institute (KNMI). Most of the nearby stations are equipped with triaxial short-period seismometers and digital recording systems. The locations of the stations are plotted on the map of Fig. 1.

In addition, high-dynamic broadband records, which were extremely useful to determine the source parameters and the local magnitudes of the Roermond earthquake sequence, have been supplied by the German Regional Seismic Network (GRSN), especially by its nearest station Bochum (BUG) about 100 km northeast of the epicenter.

Most of the aftershocks were recorded in the nearfield of the source by a temporary network of up to 29 mobile seismographs which have been installed shortly after the mainshock in the region around the epicenter. The first of the mobile stations started to operate already 5 hours after the mainshock. The monitoring and comprehensive analysis of the aftershock activity was done by a multi-national working group of seismologists from the Netherlands, Belgium, Germany and France (Camelbeeck et al. 1994).

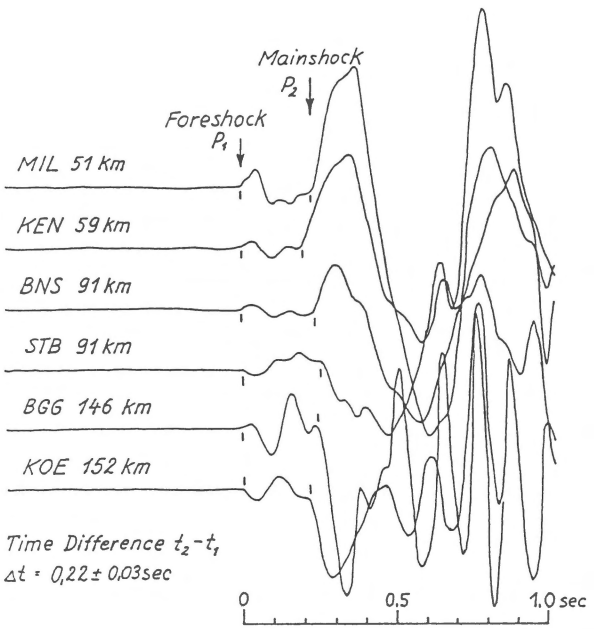

Fig. 2. P-wave signals of the Roermond earthquake recorded by the seismic station network of the university of Cologne in the Lower Rhine Embayment and in the Rhenish Massif. Seismogram traces display the vertical component of ground motion at each station. t_1 and t_2 refer to arrival times of the first and second P-wave (P_1 and P_2). Stations are listed in Table 1.

Roermond mainshock

Source complexity and hypocenter location

From P-waveforms of the Roermond earthquake (Fig. 2) recorded by digital seismic stations of the University of Cologne between 51 km and 152 km from the epicenter, it becomes clear that this earthquake was a multiple event, consisting of at least two different shocks. A smaller foreshock (event 1) was followed about 0.2 sec later by a larger second shock (event 2), which was obviously the mainshock. The observed time differences between the P-arrivals of the foreshock and the mainshock are rather constant (mean value of the time difference P_2 - P_1 = 0.22 s ± 0.03 s) and show no significant variation with azimuth or focal distance of the recording stations. Therefore, the hypocenter locations of both shocks must be nearly the same.

From the arrival times of P- and S-waves (Table 1) from 34 stations up to a distance of 153 km the origin time and the epicenter locations of the foreshock and the mainshock have been calculated with high precision (Table 2). Both epicenters are located about 5 km southwest of the city of Roermond (Fig. 3). The calculated focal depth is about 14 to 15 km. The standard error of the epicenter determination is about ± 1 km, whereas the error of the focal depth determination is somewhat larger (about ± 3 km). This is mainly due to the fact that the nearest recording station KRN is situated at a distance of 34 km from the epicenter. A focal depth for the mainshock in the range of 14 to 18 km seems to be most probable if we also take into account the results of the macroseismic focal depth estimation (Meidow & Ahorner 1994).

The calculation of the instrumental hypocenters has been performed by means of an iterative computer code ORTUNG, which was developed at our institute for use with normal MS-DOS computers. The assumed crustal velocity model (Table 3) is our standard model for the routine determination of earthquake sources in the Rhine area (Ahorner 1983).

Table 1. Arrival times of P- and S-waves used for the hypocenter calculation of the Roermond mainshock and its foreshock. Arrival times are given in seconds after 01 h 20 m UTC, April 13, 1992. The first motion direction of P-waves is denoted by C (for compression) resp. D (for dilatation). Stations marked by a star (*) are located on unconsolidated sediments of greater thickness.

Station code	Geographical coordinates		Hypocenter distance	Foreshock P-wave (P_1)	Mainshock P-wave (P_2)	S-wave
	Lat. (N))	Long. (E)	(km)	(sec)	(sec)	(sec)
KRN	50.875°	6.077°	37.4	8.86 D	–	–
VKB	50.867°	5.785°	38.1	8.99 D	–	–
ENN	50.767°	5.923°	47.2	10.38 D	–	–
EBN	50.797°	5.680°	47.3	10.51 C	–	–
KRF	50.343°	6.538°	49.1	10.70 D	–	–
MIL*	50.993°	6.559°	50.7	11.32 C	11.55 C	18.39
BOH*	50.968°	6.623°	55.7	12.26 C	12.49 C	19.90
KIR*	50.958°	6.640°	57.2	12.62 C	12.88 C	–
TGA*	50.959°	6.651°	57.9	12.82 C	13.01 C	20.66
KEN*	50.950°	6.657°	58.7	13.05 C	13.23 C	21.31
GSH	50.737°	6.377°	59.6	12.55 C	–	19.90
SIN*	50.919°	6.666°	60.6	13.40 C	13.65 C	21.00
RPM	51.472°	6.634°	61.5	12.85 C	–	20.13
DRE	50.663°	6.233°	62.2	12.85 C	13.04 C	20.07
MEM	50.609°	6.007°	64.4	13.33 C	–	21.06
LCH	50.637°	5.601°	65.3	13.38 C	–	21.38
PLH	50.005°	6.821°	66.9	13.76 C	13.98 C	21.60
STI	50.585°	5.564°	71.5	14.54 C	–	23.36
OLF	50.496°	6.421°	84.1	16.36 C	16.61 C	26.48
BNS	50.964°	7.176°	91.9	18.34 C	18.55 C	28.99
STB	50.584°	6.840°	92.0	18.55 D	18.80 D	29.25
BUG	51.446°	7.264°	99.5	18.97 C	19.19 C	30.66
WBS	50.810°	7.280°	104.3	–	19.94	
WTS	51.996°	6.810°	111.7	–	20.53	–
WIB	50.161°	5.726°	114.1	21.63 C	–	34.45
UCC	50.798°	4.359°	118.7	21.97 C	–	–
DBN*	52.102°	5.177°	116.0	–	22.50 D	–
HUM	50.193°	5.260°	119.4	22.01 C	–	–
OCH	50.371°	7.376°	136.4	23.83 D	24.00 D	–
SNF	50.512°	4.284°	138.0	–	24.71 C	–
VIA	49.936°	6.204°	139.4	24.85 C	–	–
BGG	50.206°	7.337°	147.2	25.24 C	25.48 D	43.39
KOE	50.425°	7.732°	152.7	26.01 D	26.22 D	44.81
DOU	50.096°	4.594°	153.1	–	26.54 C	45.32

From the determined hypocenters it becomes clear that the source zones of the foreshock and the mainshock are located close together and are obviously situated at the depth continuation of the Peel Boundary Fault (Fig. 4). This well-known geological feature represents a major tectonic fracture zone of the normal fault type, which dips steeply to the southwest and forms the eastern border of the Roer Valley Graben.

Local magnitude

The local magnitude of the Roermond mainshock was calculated using the displacement amplitude of eight digital stations with unclipped seismograms, situated between 60 km and 153 km from the epicenter and all located on rigid rock (Table 4). The resulting mean value of the local magnitude is $M_L = 5.9 \pm 0.1$.

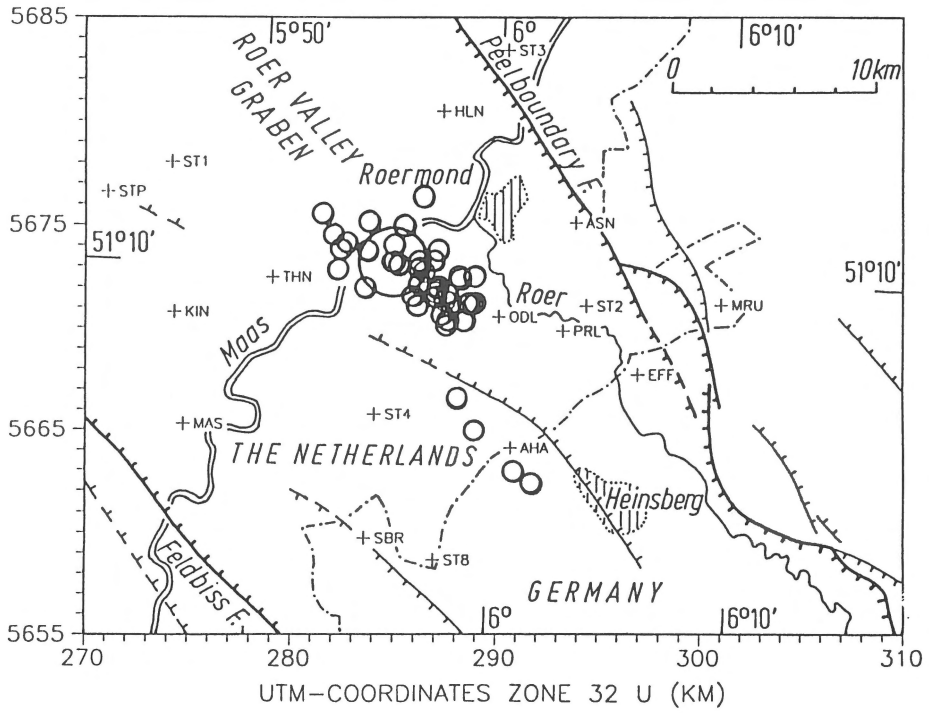

Fig. 3. Sketch map of the Roermond area with the epicenter locations of the Roermond mainshock (big circle) and its stronger aftershocks (small circles). Stations of the temporary seismic network are marked by crosses. Active faults are drawn with barbs on the downthrown side (after Ahorner 1962). Coordinates in UTM Zone 32U.

Table 2. Calculated hypocenters for the Roermond foreshock and mainshock

	Foreshock (event 1)	Mainshock (event 2)
Origin time (UTC)	01h 20m 02.6s ± 0.1s	01h 20m 02.8s ± 0.1s
Latitude North	51.168° ± 1.0km	51.170° ± 1.0km
Longitude East	5.927° ± 1.0km	5.925° ± 1.0km
Focal depth	14.0km ± 3.0km	14.6km ± 3.0km

Table 3. Crustal velocity model used for the hypocenter determination (from Ahorner 1983). The model is valid for stations located on rigid rock

Layer No.	Thickness (km)	Seismic velocity	
		P-wave (km/sec)	S-wave (km/sec)
1	1.0	5.00	2.96
2	1.0	5.50	3.25
3	1.0	5.80	3.43
4	7.0	6.00	3.55
5	9.0	6.25	3.70
6	12.0	6.90	4.08
7	–	8.10	4.76

Moho-depth 31 km (between layer 6 and 7).

For the calculation of the local magnitude the following formula deduced from Richter's original log A_o-values by converting Wood-Anderson amplitudes to ground amplitudes was used (Ahorner 1983):

$$M_L = \log(A_h) + 1.90\log(R) - 0.35 \qquad (1)$$

A_h is the maximum S-wave displacement amplitude (in 10^{-6} m) measured as the arithmetric mean from both horizontal components, and R is the hypocenter distance (in km).

Local magnitudes determined with this formula from the usual short-period seismograms agree well with the local magnitude M_L (MWA) = 5.9. This ML has been calculated for the Roermond mainshock from a Wood-Anderson simulation of the broadband records of the GRSN-Station Bochum (BUG) using the original log A_o values of Richter for an epicentral distance of 99 km.

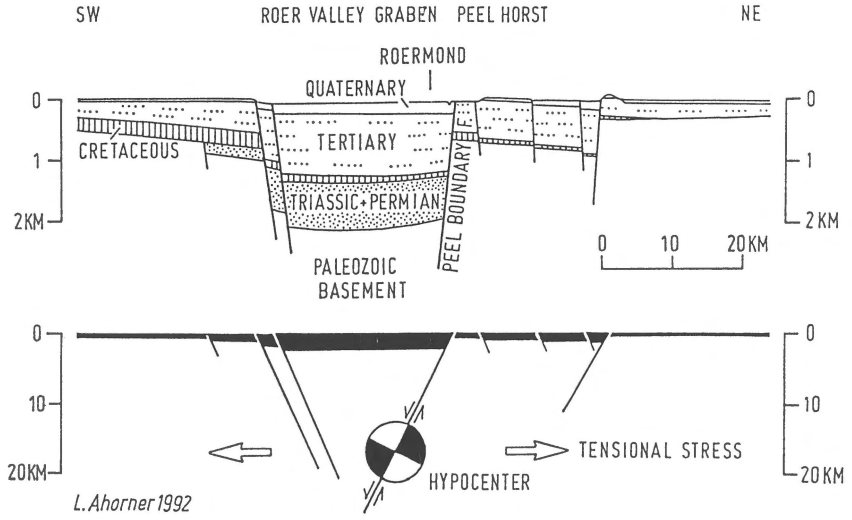

Fig. 4. Simplified geological cross-section through the Roer Valley Graben near Roermond (for location see Fig. 1). The hypocenter of the Roermond mainshock is located on the depth continuation of the Peel Boundary Fault which forms the eastern border of the Roer Valley Graben.

Table 4. Determination of the local magnitude M_L for the Roermond mainshock. M_L was calculated using equation (1), with the exception of station BUG (GRSN), where Wood-Anderson simulations of the broadband seismograms were used in connection with the original $\log(A_o)$ values of Richter (1935).

Code	Station name	Hypocenter distance (km)	Displacement amplitude (10^{-6} m)		M_L	Institution
			N-S	E-W		
GSH	Großhau	59.6	707	496	5.8	GLA Krefeld
PLH	Pulheim	66.9	567	424	5.9	GLA Krefeld
OLF	Oleftalsperre	84.1	295	399	5.9	GLA Krefeld
BUG	Bochum (GRSN)	99.5	–	–	5.9 (WA)	Univ. Bochum
WBS	Wahnbachtalsperre	104.3	337	288	6.0	GLA Krefeld
HRN	Hamm	136.0	171	127	5.9	Univ. Bochum
BGG	Burg Eltz	147.2	148	198	6.0	Univ. Cologne
KOE	Köppel	152.7	221	293	6.2	Univ. Cologne
Mean value of local magnitude M_L					5.9 ± 0.1	

Stations located on unconsolidated sediments of greater thickness give in general higher local magnitudes than those on rigid rock, due to soil amplification effects. Therefore, such stations were not used for calculating the mean value of the local magnitude. Furthermore, stations with epicentral distances greater than about 150 km have been omitted in order to avoid errors caused by uncertainties concerning the appropriate amplitude decay function for the western and central European area. The decay function for our region is probably different from that in Southern California, where Richter has determined his $\log A_o$ values.

The foreshock occurring about 0.2 s before the mainshock had a local magnitude of approximately $M_L = 4.8$. This estimation is based on the average amplitude ratio of 1:11 between the P-wave signals of the foreshock and the mainshock (Fig. 2).

Magnitudes of the Roermond mainshock calculated from teleseismic data are distinctly smaller than the local magnitude $M_L = 5.9$ determined above. The routine determination of the National Earthquake Informa-

Table 5. Source parameters of the Roermond mainshock deduced from spectra of P- and S-wave signals recorded at the stations Bensberg and Bochum. The results refer to Brune's source model.

Station	Bensberg BNS	Bochum BUG (GRSN)		Mean value
Wave type	Pg (Z)	Pg (Z)	Sg (NS)	
Seismic moment M_o (Nm)	6.5×10^{16}	8.0×10^{16}	1.5×10^{17}	9.8×10^{16}
Corner frequency f_c (Hz)	1.0	1.1	0.6	–
Source radius r_o (m)	2230	2030	2170	2200
Average dislocation d_o (cm)	13	19	30	21
Stress drop p_o (MPa)	2.5	4.2	6.4	4.4

tion Center (NEIC) at Golden, USA, based on worldwide data, leads to an average body-wave magnitude M_b = 5.5 (56 observations) and surface-wave magnitude M_s = 5.2 (16 observations). A moment magnitude of M_w = 5.3 can be calculated using the relation of Hanks & Kanamori (1979), if we assume an average seismic moment of $M_o = 9.8 \times 10^{16}$ Nm (see Table 5).

Fault-plane solution

The fault-plane solution for the Roermond mainshock derived from P-wave first motions of more than 50 local and regional seismic stations up to a distance of about 600 km from the epicentre is well defined (Fig. 5). The solution presented has been worked out already a few days after the earthquake (Ahorner 1992). Similar results have been achieved later by Pelzing (1992, 1994), Paulssen et al. (1992), Camelbeeck et al. (1994) and others. Fault-plane solutions obtained by the inversion of surface waveforms recorded by the German Regional Seismic Network (Braunmiller et al. 1994) and of teleseismic P-wave signals (Ahorner & Choy 1993) confirm the solution based on local and regional first motions.

The focal mechanism of the Roermond mainshock is clearly of the dip-slip type, with one fault-plane (plane a) striking NW-SE (124°) and dipping 68° SW, and the other (plane b) striking in the same way and dipping 22° NE. The T axis (tension axis) is orientated in SW-NE direction (214°) and dips 23° SW. The P axis (pressure axis) is nearly vertical. The focal dislocation corresponds to a pure normal fault movement controlled by a SW-NE crustal tension. If we take into account the geological situation in the focal region (Fig. 4) and the spatial distribution of the aftershocks (Figs 10, 11), then the first fault-plane (plane a) is most probably the real fracture plane along which the seismotectonic shear dislocation occurred.

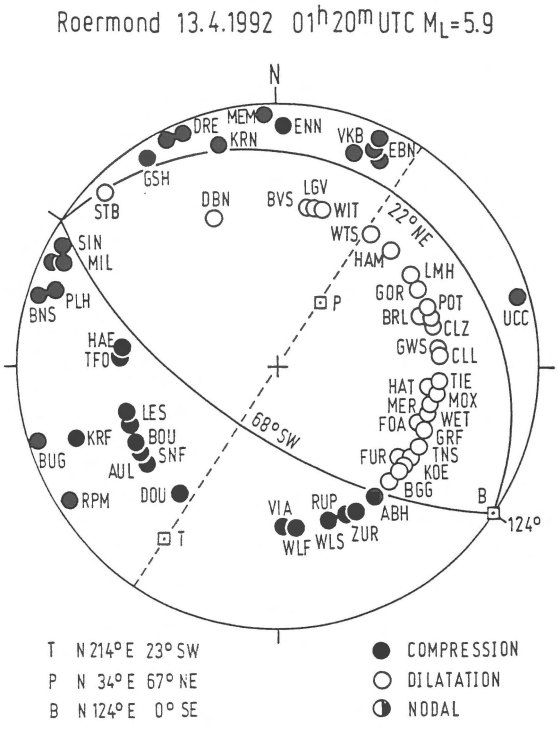

Fig. 5. Fault-plane solution for the Roermond mainshock based on P-wave first motions from local and regional records identified by station code (after Ahorner 1992). Equal-area projection of the lower hemisphere. Take-off angles of the ray paths were calculated using the crustal velocity model of Table 3. P, T and B denote Pressure, Tension and Neutral axis, respectively.

The decribed type of dislocation in combination with trivial geometrical considerations leads to the conclusion that the focal process of the Roermond mainshock was connected to an extensional seismotectonic block movement along the SW-dipping Peel Boundary

Fault (Peelrandbruch). The southwestern fault block (Roer Valley Graben) moved down with respect to the northeastern block (Peel Horst). Some difficulties arise with the strike directions of the focal plane (124°) and the near-surface fault trace (about 145°), which are not exactly the same. We have no satisfying explanation at present for this discrepancy. One possible explanation might be that the local strike direction of the Peel Boundary Fault varies slightly with depth.

The Peel Boundary Fault crops out at the earth's surface about 8 km east of the epicenter (Figs 3, 4). From geological, geodetical and seismological evidence it is well known that this major Cenozoic structural feature is still active as a normal fault zone in Quaternary and Recent times (Ahorner 1962, 1968; Geluk et al. 1994; Van den Berg 1994; Van den Berg et al. 1994). The total vertical throw at the base of the Quaternary deposits amounts up to 170 to 180 m. Even near-surface layers of Late Pleistocene and Holocene age are dislocated up to 10 m. High-precision levellings indicate a recent fault creep in the order of 1 mm per year.

Seismotectonic source parameters

In order to get an impression of size and amount of the source process of the Roermond mainshock, the seismotectonic source parameters have been estimated from the Fourier displacement spectra of P- and S-waves recorded at the seismic network of the University of Cologne. Spectra were corrected for instrumental response and anelastic energy absorption. Q-values between 300 and 500 have been used for ray paths within crustal rocks. As an example the P-wave displacement spectrum for the station Bensberg (BNS) is displayed in Fig. 7; it shows a clear corner frequency at 1.0 Hz. In addition, the body wave spectra of the broadband records of the GRSN-station Bochum (BUG) have been analyzed, with similar results with regard to the corner frequency of the source (Fig. 8).

Based on the physical source model of Brune (1970, 1971) the average source parameters listed in Table 5 were calculated for the Roermond mainshock. The results agree well with the source parameters determined by Camelbeeck et al. (1994) from local and regional data and by Scherbaum (1994) and Braunmiller et al. (1994) from GRSN data. From the inversion of teleseismic signals of the Roermond mainshock, carried out at the Geological Survey in Denver, USA, comparable estimates for the source parameters have been obtained (seismic moment 6.6×10^{16} Nm,

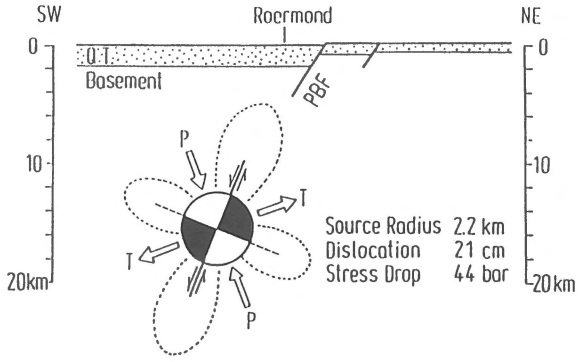

Fig. 6. Schematic cross-section showing the hypocenter location and the focal mechanism of the Roermond mainshock with respect to the Peel Boundary Fault (PBF). Pressure axis (P) and tension axis (T) of the focal mechanism are denoted by arrows. Dashed contour lines illustrate the shear-wave radiation pattern of the source. High-amplitude ground motion was produced at the Earth's surface northeast of the epicenter. Unconsolidated Quaternary and Tertiary deposits (QT) above the consolidated substratum are dotted.

static stress drop 2.1 MPa, rise time $\approx$ 1.0 sec, source size from rise time $\approx$ 2500 m; Ahorner & Choy (1993).

The source parameters calculated for the Roermond mainshock fit in well with the generalized relationships between local magnitude and specified source parameters derived by Ahorner (1983) from smaller earthquakes occurring in the period 1977–1982 in the Lower Rhine Embayment and the adjoining Rhenish Massif. For example, the corresponding magnitude vs. seismic moment relation is shown in Fig. 9. This relation covers, in western and central Europe, the local magnitude range of $1 \leq M_L \leq 6$.

The results of our investigations of the source process of the Roermond mainshock can be summarized as illustrated in the schematic cross section of Fig. 6. About 14 to 18 km below the surface an extensional seismotectonic shear dislocation of the dip-slip type occurred at the depth continuation of the Peel Boundary Fault. Along the active fault-plane the western block (Roer Valley Graben) moved down with respect to the eastern block (Peel Horst). The activated fault plane is assumed to have a circular shape according to Brune's (1970, 1971) source model and measures 4 to 5 km in diameter covering an area of approximately 15 km^2. The average displacement along this fault segment was about 21 cm; the static stress drop connected with the seismotectonic dislocation was in the order of 4.4 MPa (44 bar).

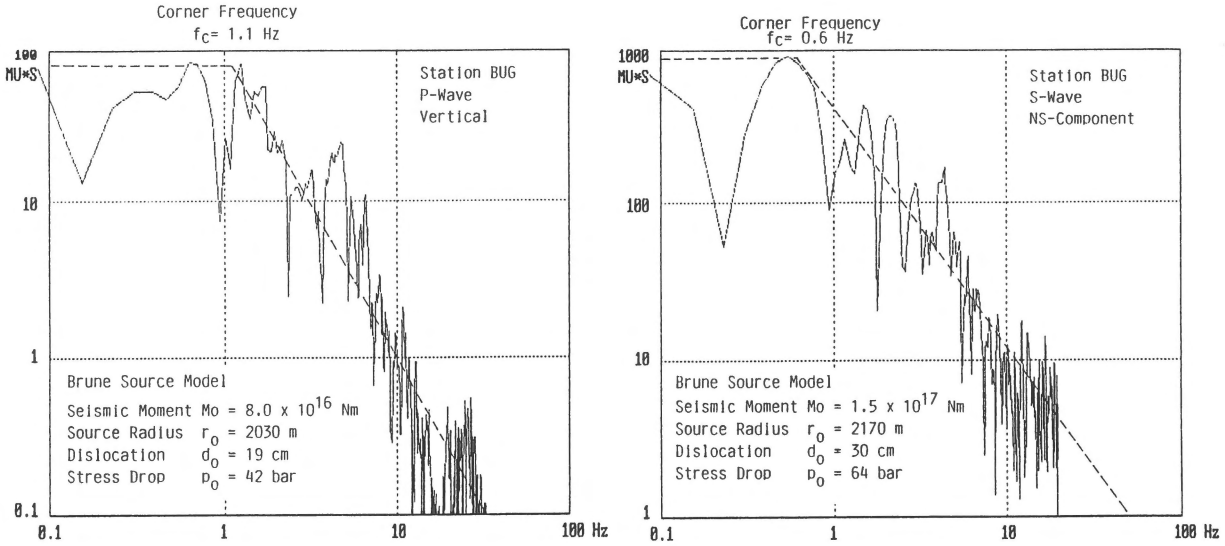

Fig. 8. Fourier displacement spectra derived from the P-wave (left) and SH-wave signals (right) of the Roermond mainshock recorded at the GRSN broadband station Bochum (BUG). Source parameters were calculated using the physical source model of Brune (1970, 1971). Amplitude density as in Fig. 7.

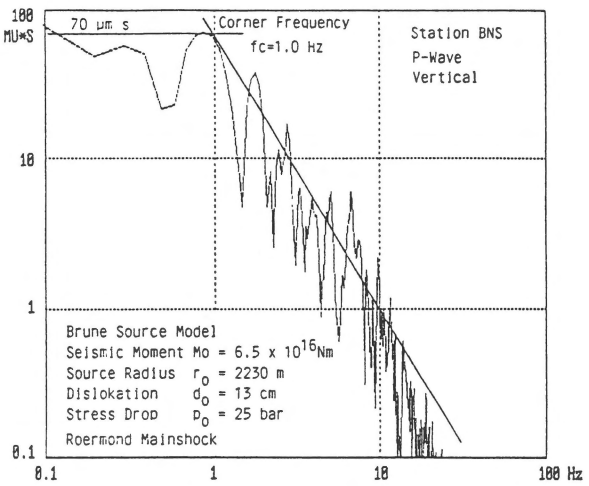

Fig. 7. Fourier displacement spectrum derived from the P-wave signal of the Roermond mainshock recorded at the station Bensberg (BNS). Source parameters were calculated using the physical source model of Brune (1970, 1971). Amplitude-density is given in microns × seconds (MU * S).

Aftershock sequence

The Roermond mainshock was followed until the middle of May 1992 by more than 200 aftershocks. Most of these occurred during the first two days. Some 29 aftershocks had local magnitudes of $M_L \geq 2$, with four

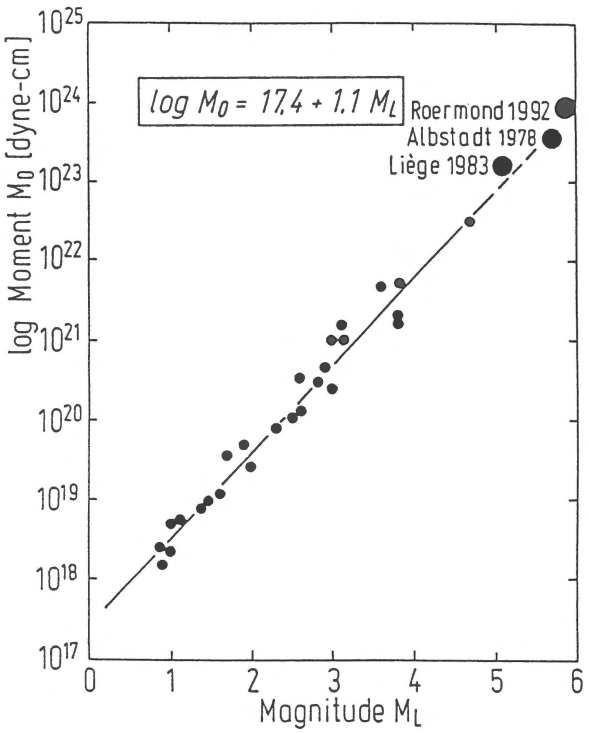

Fig. 9. Relation between local magnitude and seismic moment found by Ahorner (1983) for earthquakes occurring 1977–1982 in the Lower Rhine area and in the Rhenish Massif. The damaging earthquakes of Albstadt 1978, Liège 1983 and Roermond 1992 fit in with the generalized relationship deduced from the smaller events.

exceeding the magnitude $M_L = 3$ level. The strongest event, with magnitude $M_L = 3.8$, was released on April 14, 1 h 06 m UTC, in the region of Immendorf near Geilenkirchen, about 30 km southeast of Roermond. This shock was felt in Germany over a rather large area. The macroseismic radius was about 100 km and the epicentral intensity V MSK (Meidow & Ahorner 1994).

Most of the events following the Roermond mainshock occurred in the vicinity of the mainshock hypocenter (Camelbeeck et al. 1994). But a considerable number of events was released at greater distance in various parts of the Lower Rhine Embayment, e.g. in the region east and northeast of Aachen (Prinz et al. 1994) and even in the region south of Cologne. Obviously, these distant events cannot be interpreted as normal aftershocks. They were triggered by crustal stress changes resulting from dynamic forces, which have been induced by the Roermond mainshock in those parts of the Lower Rhine Embayment where critical stress conditions were already present.

Within the multi-national working group (Camelbeeck et al. 1994), the research work of our institute focused on the precise determination of the hypocenter locations, focal mechanisms and source parameters of the stronger aftershocks with local magnitudes $M_L \geq 2.0$, which have been recorded by the station network of the University of Cologne. Table 2 gives a list of events investigated by our institute. The listed local magnitudes are the mean values from three or more stations. Equation (1) was used for the magnitude calculation.

The hypocenter locations were determined using the computer code ORTUNG and specified travel time corrections for P- and S-arrivals at different stations. The travel time corrections for the permanent stations were deduced from the time residuals resulting during the mainshock location procedure. The mainshock was in this case used as a master-event. Local travel time corrections for the temporary stations operating in the epicentral area after the mainshock were calculated accounting for the fact that in the Roer Valley Graben a thick low-velocity graben fill is present above the basement rocks. This sedimentary cover is up to 1500 thick and consists of unconsolidated Tertiary and Quaternary deposits (Geluk et al. 1994). The average seismic velocities within the sedimentary cover were assumed to be Vp = 2000 m/s for P-waves and Vs = 750 m/s for S-waves, according to the results of seismic borehole measurements in various parts of the Lower Rhine Embayment (Ahorner & Budny 1985).

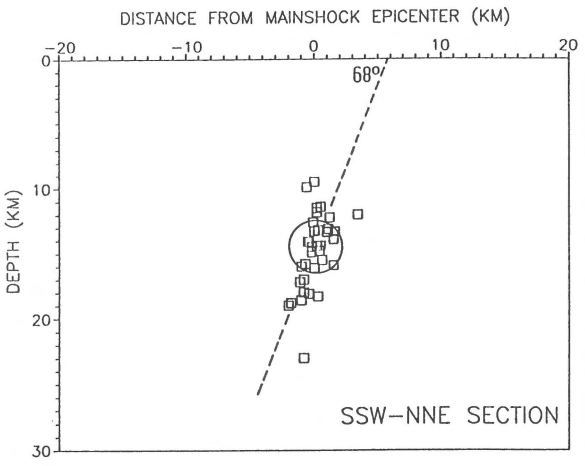

Fig. 10. Cross-section perpendicular to the strike direction of the focal zone of the 1992 Roermond earthquakes. The mainshock hypocenter projection is marked by a circle. Hypocenter projections of aftershocks are denoted by squares.

The horizontal errors of the calculated aftershock hypocenters are in general less than ± 1 km, with associated travel time residuals smaller than ± 0.1 s (see Table 2). The vertical errors are larger (up to ± 9 km) for aftershocks during the first five hours after the mainshock. When the first mobile stations started to operate in the epicentral area in the early morning hours of April 13, the depth control for aftershock sources became much better with vertical location errors of about ± 1 km.

The spatial distribution of the aftershock hypocenters in the vicinity of the mainshock source is illustrated by the epicenter map (Fig. 3) and two vertical cross-sections, which are arranged SSW-NNE and WNW-ESE, perpendicular and parallel to the fault-plane of the mainshock (Figs 10, 11). From the clustering of the aftershock hypocenters it is evident that the active fault zone generating most of the Roermond earthquakes trends NW-SE and dips steeply to the southwest. This result agrees with the seismotectonic interpretation of the fault-plane solution of the mainshock (Figs 5, 6). The focal depths of the aftershocks range between 10 and 23 km below the surface. The mainshock hypocenter is located near the center of the aftershock area, which measures about 10 km in diameter.

Fault-plane solutions for the aftershocks indicate predominantly dip-slip mechanisms along NW-SE trending fault-planes, just like the mainshock. This has also been noticed by other investigators (Camel-

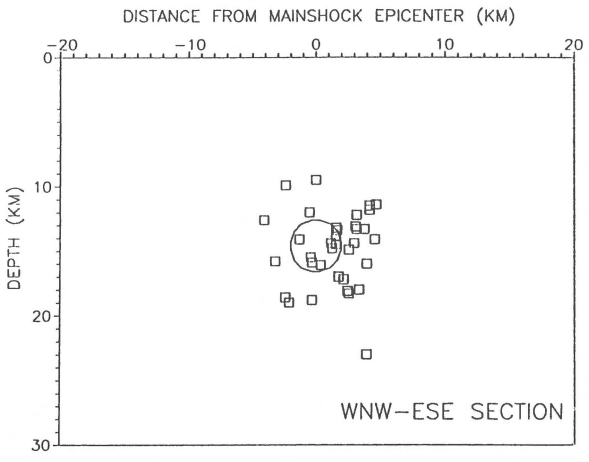

Fig. 11. Cross-section parallel to the strike direction of the focal zone of the 1992 Roermond earthquakes. The mainshock hypocenter projection is marked by a circle. Hypocenter projections of aftershocks are denoted by squares.

beeck et al. 1994). In a few cases, a combination of dip-slip and strike-slip movement or an almost pure strike-slip movement can be proven. Examples of well-defined fault-plane solutions for the stronger events following the Roermond mainshock are illustrated in Fig. 12. The fault-plane solutions in the upper part of the figure represent true aftershocks occurring during the first six hours in the vicinity of the mainshock hypocenter. The fault-plane solutions in the lower part of the figure are from events released about 24 hours after the mainshock and at greater distance from the mainshock source in the region northeast and east of Aachen. The solution for the magnitude 3.8 event near Immendorf (about 30 km southeast of Roermond) illustrates a clear tensional oblique-slip dislocation along a fault-plane striking NNW-SSE (171°) or WNW-ESE (104°). On the other hand, the solution for the magnitude 2.8 event occurring approximately 30 minutes later near Eschweiler (about 45 km SE of Roermond) shows a pure dip-slip movement along a NW-SE trending fault-plane. In all fault-plane solutions exemplified in Fig. 12 the tension axes (T-axes) are directed SW-NE and nearly horizontal. This is typical for almost all reliable fault-plane solutions of the Roermond earthquake sequence. The remarkable constancy of the direction of T-axes has also been emphasized by Camelbeeck et al. (1994).

In order to complete our knowledge on the Roermond earthquake sequence a comprehensive study of the seismotectonic source parameters of the aftershocks has been carried out at our institute by Feind (1993). These investigations are based on the Fourier displacement spectra of P- and S-waves recorded by the seismic station network of the University of Cologne. The spectral parameters, corrected for geometrical spreading, average radiation pattern, surface reflection and anelastic absorption (assuming Q_P = 700 and Q_S = 600 for crustal ray paths), were interpreted using the physical source model of Brune (1970, 1971). The mean source parameters determined for the stronger aftershocks are listed in Table 5. A graph showing the relation between seismic moment and local magnitude for 19 aftershocks is displayed in Fig. 13. The relation found for the Roermond aftershock sequence is similar to that of Fig. 9, which has been deduced from earthquakes in the Lower Rhine Embayment and in the adjoining Rhenish Massif in the period 1977–1982 (Ahorner 1983).

Seismotectonic setting of the Roermond earthquake

The 1992 Roermond earthquake is a typical intraplate tectonic earthquake, occurring in the western part of the Eurasian lithospheric plate far away from its borders. The main conclusions about this earthquake fit well into the known tectonic setting of the Lower Rhine Embayment and the general pattern of seismotectonic dislocations in the central European area (Ahorner 1970, 1983, 1985, 1993; Ahorner et al. 1983).

Two essential factors are controlling the seismotectonic block movements in western and central Europe. The first is a wide-spread regional stress field within the earth's crust which is characterized by a rather uniform trend of the maximum horizontal stress in NW-SE direction and the minimum horizontal stress in SW-NE direction (Ahorner et al. 1983; Baumann & Illies 1983; Plenefisch & Bonjer 1994; Grünthal & Stromeyer 1994). It is generally believed that this intraplate stress field is caused by large-scale plate tectonics, especially by the southeastward drift of the European plate relative to the African plate and the dynamical interaction between these two plates. The second controlling factor is the post-Hercynian block mosaic in the western and central European area, especially the existence of deep-reaching major fracture zones like the border faults of the Rhine Graben system, which form distinct zones of crustal weakness (Ziegler 1992, 1994).

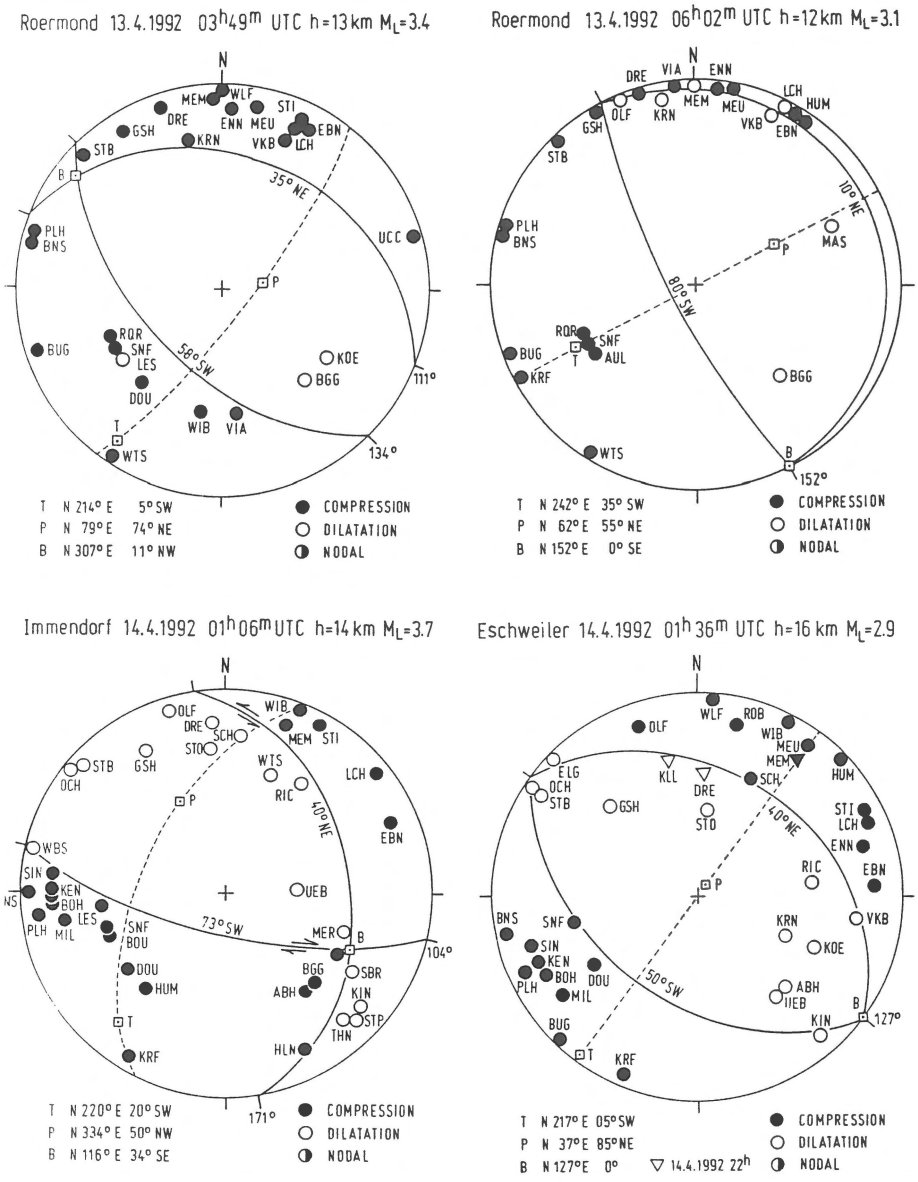

Fig. 12. Fault-plane solutions for stronger aftershocks released in the vicinity of the mainshock hypocenter (above) and for seismic events induced by the Roermond earthquake at greater distance (below). Equal-area projection of the lower hemisphere. The source coordinates and other basic data of the events are given in Table 6. The measurements are identified by the station code (Table 1).

Under the influence of the present-day stress field, characteristic seismotectonic block movements are going on along pre-existing zones of crustal weakness, which can be described by the rather simple deformation model proposed by Ahorner (1985). This model explains the predominance of specific types of earthquake focal mechanisms in different parts of the western and central European area. In the Lower Rhine Embayment, which forms the northwestern segment of the Rhine graben system, the prevailing focal mechanism type is the extensional dip-slip (normal fault) along fault-planes trending NW-SE, perpendicular to the direction of the minimum horizontal crustal stress.

The focal mechanisms obtained for the Roermond earthquake sequence fit well into the large-scale seismotectonic deformation model mentioned before. Almost all reliable fault-plane solutions of the sequence, including the solution for the mainshock, present an extensional dislocation with the tension axis

Table 6. Basic data of the Roermond earthquake sequence determined by the Department of Earthquake Geology of the University of Cologne. Only stronger events with local magnitudes $M_L \geq 2$ are listed. SD refers to the standard deviation.

Region	Date	Origin time (UTC)	Epicenter		SD (km)	Depth (km)	SD (km)	M_L
			lat. N	long. E				
Roermond	13.4.1992	01h 20m 02.6s	51.168°	5.927°	± 1	14.0	± 3	(4.8)
Roermond	13.4.1992	01h 20m 02.8s	51.170°	5.925°	± 1	14.6	± 3	5.9
Roermond	13.4.1992	01h 22m 52.5s	51.073°	6.016°	± 1	16.6	± 9	3.1
Roermond	13.4.1992	01h 33m 32.3s	51.158°	5.908°	± 1	18.8	± 3	2.3
Roermond	13.4.1992	02h 02m 24.0s	51.156°	5.957°	± 1	18.1	± 5	2.1
Roermond	13.4.1992	02h 08m 20.8s	51.155°	5.941°	± 1	17.0	± 5	2.1
Roermond	13.4.1992	03h 03m 26.3s	51.170°	5.928°	± 1	9.5	± 3	2.3
Roermond	13.4.1992	03h 17m 49.6s	51.190°	5.876°	± 1	12.6	± 9	2.1
Roermond	13.4.1992	03h 41m 27.2s	51.145°	5.978°	± 1	14.1	± 5	2.3
Roermond	13.4.1992	03h 49m 42.6s	51.154°	5.963°	± 1	13.3	± 4	3.4
Eschweiler	13.4.1992	04h 32m 48.0s	50.837°	6.250°	± 1	13.8	± 1	2.3
Heinsberg	13.4.1992	04h 37m 45.6s	51.075°	6.028°	± 1	16.4	± 2	2.1
Heinsberg	13.4.1992	05h 20m 45.4s	51.091°	5.981°	± 1	17.1	± 9	2.6
Roermond	13.4.1992	05h 25m 29.9s	51.145°	5.966°	± 1	23.0	± 6	2.1
Roermond	13.4.1992	06h 02m 11.5s	51.153°	5.980°	± 1	11.5	± 2	3.1
Roermond	13.4.1992	06h 16m 35.0s	51.158°	5.964°	± 1	14.4	± 1	2.4
Roermond	13.4.1992	06h 33m 40.1s	51.154°	5.984°	± 1	11.4	± 1	2.6
Roermond	13.4.1992	21h 50m 02.1s	51.176°	5.957°	± 1	13.9	± 2	2.0
Roermond	13.4.1992	22h 59m 21.6s	51.158°	5.957°	± 1	14.9	± 1	2.1
Immendorf	14.4.1992	01h 06m 46.4s	50.941°	6.175°	± 1	13.8	± 1	3.8
Eschweiler	14.4.1992	01h 36m 23.4s	50.830°	6.231°	± 1	16.2	± 1	2.8
Roermond	14.4.1992	02h 31m 07.0s	51.164°	5.974°	± 1	12.2	± 1	2.3
Roermond	14.4.1992	12h 41m 39.9s	51.181°	5.884°	± 1	15.8	± 1	2.7
Roermond	14.4.1992	12h 56m 32.0s	51.166°	5.948°	± 1	13.2	± 3	2.9
Roermond	16.4.1992	14h 07m 15.9s	51.175°	5.890°	± 1	18.6	± 1	2.1
Eschweiler	20.4.1992	16h 50m 08.7s	50.815°	6.215°	± 1	16.9	± 2	2.2
Godorf	20.4.1992	19h 52m 04.6s	50.858°	6.978°	± 1	12.6	± 2	2.0
Roermond	24.4.1992	10h 35m 27.0s	51.165°	5.984°	± 1	13.3	± 1	2.1
Roermond	2.5.1992	08h 50m 02.7s	51.163°	5.974°	± 1	13.2	± 1	2.4
Roermond	15.5.1992	19h 33m 26.8s	51.171°	5.955°	± 1	13.5	± 1	2.9
Aldenhoven	17.5.1992	09h 25m 57.6s	50.887°	6.296°	± 1	5.0	± 5	2.1

(T-axis) arranged sub-horizontal in SW-NE direction (Figs 14, 15). This remarkable constancy in the spatial arrangement of T-axes has been proven already by Ahorner & Pelzing (1983) for earthquakes occurring in the Roer Valley Graben and its vicinity, prior to the 1992 Roermond earthquake sequence.

From these findings we may conclude that tensional forces, acting in SW-NE direction in the crustal basement of the Lower Rhine Embayment, are responsible for the origin of the 1992 Roermond earthquake sequence and of other tectonic earthquakes in the Roer Valley Graben. The tensional crustal deformation in SW-NE direction is combined with a compression in NW-SE direction. This can be proven by in situ stress measurements (Baumann & Illies 1983; Fig. 15) and also by earthquake focal mechanisms (Ahorner 1983; Ahorner et al. 1983; Ahorner & Pelzing 1983; Plenefisch & Bonjer 1994).

The tensional graben tectonics of the Lower Rhine Graben, which started already in the Early Tertiary and continued until the Quaternary, is going on under the influence of the present-day stress field. NW-SE trending crustal fracture zones like the Peel Boundary Fault, which are arranged perpendicular to the tensional stress direction, are still active as normal faults. Graben zones bordered by such faults, like the Roer Valley Graben, are subsiding with respect to the neighbouring horst zones. The resulting concentrations of shear stress at

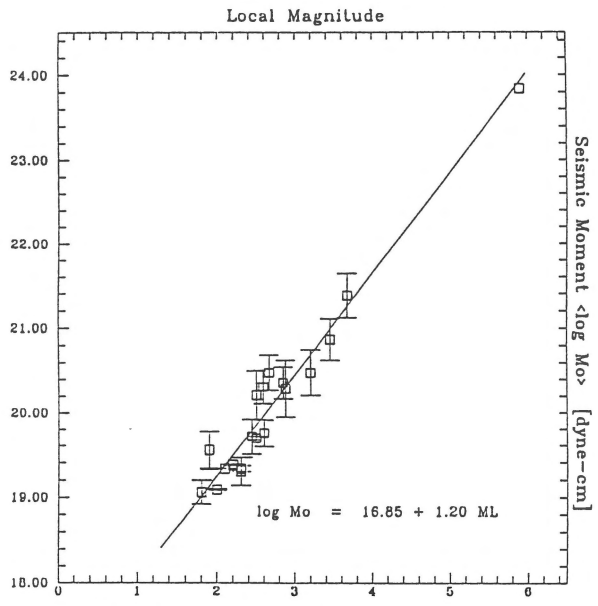

Fig. 13. Seismic moment $\log(M_o)$ versus local magnitude M_L for the mainshock and 19 aftershocks of the Roermond earthquake sequence. The solid line is a least squares fit to the data given by the equation shown (after Feind 1993).

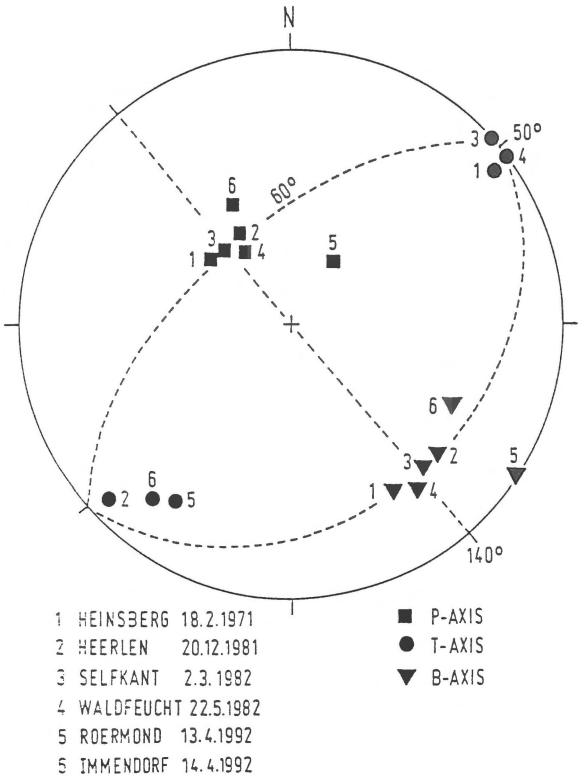

Fig. 14. Stereographic plot showing the spatial distribution of tension axes (T-axes) and pressure axes (P-axes) from fault-plane solutions of earthquakes occurring since 1971 in the Roer Valley Graben, including the Roermond mainshock and its stronger aftershocks (from Ahorner & Pelzing 1983; modified).

the border zones of the moving crustal blocks must be regarded as primary causes of tectonic earthquakes in the Lower Rhine Embayment.

In summary, a large-scale seismotectonic deformation model, proposed for the western and central European area more than two decades ago, can explain the origin of the 1992 Roermond earthquake quite well. Therefore, this earthquake, centered at the depth continuation of the Peel Boundary Fault was not surprising for seismologists, neither in its general location nor in its time and size. A comparatively large tectonic earthquake, ranging in magnitude up to $M_L \approx 6$, could be expected in the Roermond area sooner or later, if one takes into account the specific geological and geodetical characteristics of the Peel Boundary Fault and the seismological experience of the past. Of course, it was not possible to prognosticate the exact time and place of such an event.

On account of our scientific knowledge prior to the 1992 Roermond earthquake the Peel Boundary Fault must be regarded as a very active crustal fracture zone capable of producing strong earthquakes. The Peel Boundary Fault undoubtedly forms one of the most potential seismoactive features not only in the Lower Rhine Embayment, but in the whole western and central European region. Consequently, the Roermond area has been judged on existing seismic risk maps (e.g. Ahorner et al. 1976) as a region of comparatively high seismic risk, where damaging earthquakes up to intensity VII MSK or even higher must be expected. Based on probabilistic seismic hazard assessments for the Lower Rhine Embayment, statistical occurrence rates in the order of 10^{-3} per year have been prognosticated for macroseismic intensities $\geq$ VII MSK at sites in the Roermond area (Ahorner & Rosenhauer 1975; De Crook 1993; Rosenhauer & Ahorner 1994). The recent Roermond earthquake has demonstrated convincingly that these prognoses were realistic.

Acknowledgements

The author thanks all colleagues and institutions who have supplied seismic data concerning the Roermond earthquake sequence. Special thanks to Eberhard Schmedes from the Geophysical Observato-

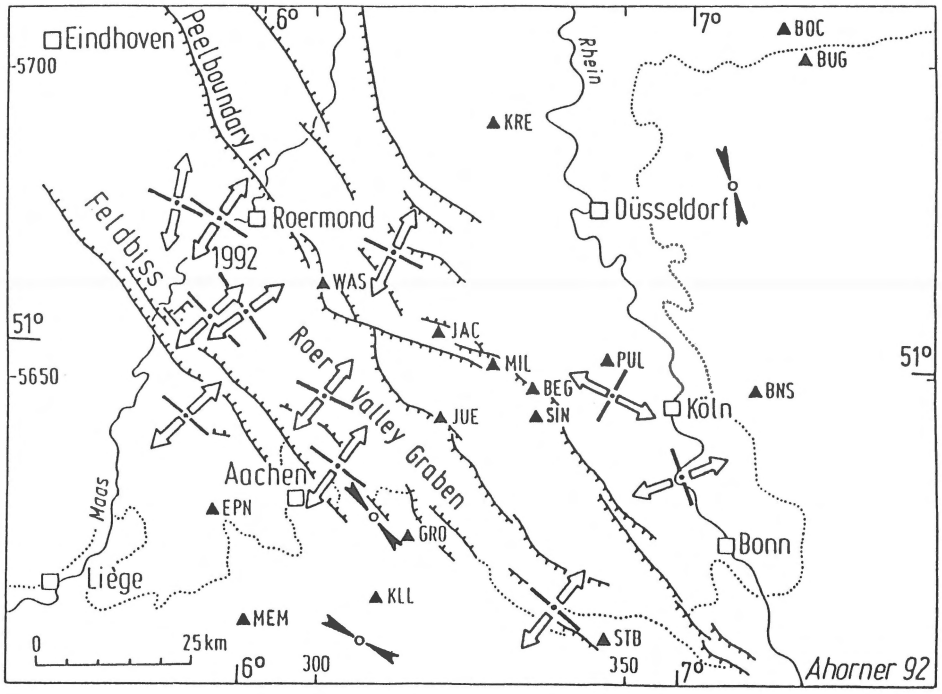

Fig. 15. Seismotectonic sketch map of the Lower Rhine Embayment (from Ahorner & Pelzing 1983; modified). Open arrows denote the direction of tension axes (T-axes) for earthquake focal mechanisms of the dip-slip type, including those of the Roermond earthquake sequence. The tension axes are arranged predominantly SW-NE, indicating that the Lower Rhine Embayment and especially the Roer Valley Graben are nowadays mainly affected by SW-NE extensional forces. Solid arrows denote δ_1-directions (maximum compressive horizontal stress) from in situ stress measurements. Active normal faults are drawn with barbs at the downthrown side. Triangles give the locations of permanent seismic stations.

Table 7. Source parameters of stronger aftershocks of the Roermond earthquake. Listed are the mean values of source parameters which were derived from the spectra of Pg and Sg signals recorded by three or more seismic stations of the Cologne network (from Feind 1993).

Event Location	Date	Time	Local magnitude M_L	Seismic moment M_o (Nm)	Source radius r_o (m)	Stress drop p_o (MPa)	Average dislocation d_o (cm)
Roermond	13.4.	3h 49m	3.4	7.3×10^{13}	194	3.5	1.9
Roermond	13.4.	6h 02m	3.1	3.0×10^{13}	171	2.6	1.1
Roermond	13.4.	21h 50m	2.0	3.6×10^{12}	172	0.4	0.1
Immendorf	14.4.	1h 06m	3.8	2.4×10^{14}	257	5.6	3.1
Eschweiler	14.4.	1h 36m	2.8	3.0×10^{13}	229	1.5	0.7
Roermond	14.4.	2h 31m	2.3	5.1×10^{12}	143	1.4	0.4
Roermond	14.4.	12h 41m	2.7	2.0×10^{13}	230	0.6	0.3
Roermond	14.4.	12h 56m	2.9	2.3×10^{13}	178	2.0	0.8

ry in Fürstenfeldbruck for making available Wood-Anderson simulations of the GRSN stations. Critical comments of two unknown reviewers, which led to an improvement of the manuscript, are gratefully acknowledged.

References

Ahorner, L. 1962 Untersuchungen zur quartären Bruchtektonik der Niederrheinischen Bucht – Eiszeitalter und Gegenwart 13: 24–105

Ahorner, L. 1968 Erdbeben und jüngste Tektonik im Braunkohlenrevier der Niederrheinischen Bucht – Z. Deutsch. Geol. Ges. 118: 150–160

Ahorner, L. 1970 Seismotectonic relations between the graben zones of the Upper and Lower Rhine valley. In: H.J. Illies & St. Müller (eds): Graben Problems – Schweizerbart, Stuttgart: 155–166

Ahorner, L. 1983 Historical seismicity and present-day microearthquake activity of the Rhenish massif, Central Europe. In: K. Fuchs et al. (eds): Plateau Uplift – Springer-Verlag, Berlin: 198–221

Ahorner, L. 1985 The general pattern of seismotectonic dislocations in Central Europe as the background for the Liège Earthquake on November 8, 1983. In: P. Melchior (ed.): Seismic Activity in Western Europe – D. Reidel Publishing Co.: 41–56

Ahorner, L. 1992 Das Erdbeben bei Roermond am 13. April 1992 und die daraus zu ziehenden Lehren für das Erdbebengefährdungspotential im Rheinland – Mittlg. Deutsch. Geophysik. Ges. 1/2: 51–57

Ahorner, L. 1993 Seismicity and seismotectonics of the Lower Rhine Embayment as part of the Rhine Graben system in Central Europe. A review of the seismological background of the Roermond earthquake. In: 'The Roermond earthquake of April 13, 1992, seismotectonic and seismic hazard in the Rhine Graben system', KNMI Workshop, Veldhoven, The Netherlands, January 20–22, Program and abstracts: 33

Ahorner, L. & M. Budny 1985 Seismische Bestimmung der bodendynamischen Kennwerte von oberflächennahen Schichten in Erdbebengebieten der Niederrheinischen Bucht. In: K.-H. Heitfeld (ed.): Ingenieurgeologische Probleme im Grenzbereich zwischen Locker- und Festgsteinen – Springer Verlag, Berlin: 560–582

Ahorner, L. & G. Choy 1993 Fault plane solutions and source parameters of the 1992 Roermond mainshock and its stronger aftershocks from regional and teleseismic data. In: 'The Roermond earthquake of April 13, 1992, seismotectonics and seismic hazard in the Rhine Graben system', KNMI Workshop, Veldhoven, The Netherlands, January 20–22, Program and abstracts: 25

Ahorner, L. & R. Pelzing 1983 Seismotektonische Herdparameter von digital registrierten Erdbeben der Jahre 1981 und 1982 in der westlichen Niederrheinischen Bucht – Geol. Jb. E 26: 35–63

Ahorner, L. & W. Rosenhauer 1975 Probability distribution of earthquake accelerations with applications to sites in the Northern Rhine area, Central Europe – J. Geophys. 41: 581–594

Ahorner, L., J.A. Flick, J.M. van Gils, A.R. Ritsema & G. Houtgast 1976 First draft of an earthquake zoning map of Northwest Germany, Belgium, Luxembourg and The Netherlands. In: A.R. Ritsema (ed.): Proc. European Seismological Commission Symposium 'On earthquake risk for nuclear power plants', Luxembourg 20–22 October 1975 – Royal Neth. Meteor. Inst., De Bilt, publ. 153: 39–41

Ahorner, L., B. Baier & K.-P. Bonjer 1983 General pattern of seismotectonic dislocations and the earthquake-generating stress field in Central Europe between the Alps and the North Sea. In: K. Fuchs et al. (eds): Plateau Uplift – Springer Verlag, Berlin: 187–197

Baumann, H. & J.H. Illies 1983 Stress field and strain release in the Rhenish Massif. In: K. Fuchs et al. (eds): Plateau Uplift – Springer Verlag, Berlin: 177–186

Braunmiller, T., T. Dahm & K.-P. Bonjer 1994 Source mechanism of the April 1992 Roermond earthquake, the Netherlands, from inversion of regional surface waves – Geol. Mijnbouw, this issue

Brune, J.N. 1970 Tectonic stress and the spectra of seismic shear waves from earthquakes – J. Geophys. Res. 75: 4997–5009

Brune, J.N. 1971 Correction – J. Geophys. Res. 76: 5002

Camelbeeck, T., T. van Eck, R. Pelzing, L. Ahorner, J. Loohuis, H.W. Haak, P. Hoang-Trong & D. Hollnack 1994 The 1992 Roermond earthquake, the Netherlands, and its aftershocks – Geol. Mijnbouw, this issue

De Crook, Th. 1993 Probabilistic seismic hazard assessment for The Netherlands – Geol. Mijnbouw 72: 1–13

Feind, H. 1993 Seismotektonische Herdparameter der Nachbeben des Roermond-Erdbebens am 13. April 1992 in der Niederrheinischen Bucht – Diploma Thesis, Geological Institute, University of Cologne, 155 pp

Geluk, M.C., E.J.Th. Duin, M. Dusar, R.H.B. Rijkers, M.W. van den Berg & P. van Rooijen 1994 Stratigraphy and tectonics of the Roer Valley Graben – Geol. Mijnbouw, this issue

Grünthal, G. & D. Stromeyer 1994 The crustal stress field in central Europe sensu lato and its quantitative modelling – Geol. Mijnbouw, this issue

Haak, H.W., J.A. van Bodegraven, R. Sleeman, R. Verbeiren, L. Ahorner, H. Meidow, G. Grünthal, P. Hoang-Trong, R.M.W. Musson, P. Henni, Z. Schenkova & R. Zimova 1994 The macroseismic map of the 1992 Roermond earthquake – Geol. Mijnbouw, this issue

Hanks, Th.C. & H. Kanamori 1979 A moment magnitude scale – J. Geophys. Res. 84: 2348–2350

Houtgast, G. 1992 Catalogus Aardbevingen in Nederland – Kon. Ned. Meteor. Inst., publ. 179, 166 pp

Meidow, H. & L. Ahorner 1994 Macroseismic effects in Germany of the 1992 Roermond earthquake and their interpretation – Geol. Mijnbouw, this issue

Paulssen, H., B. Dost & T. van Eck 1992 The April 13, 1992 earthquake of Roermond (The Netherlands); first interpretation on the NARS seismograms – Geol. Mijnbouw 71: 91–98

Pelzing, R. 1992 Das Erdbeben von Roermond 13. April 1992 – Veröff. Geolog. Landesamt Nordrhein Westfalen: 1–16

Pelzing, R. 1994 Source parameters of the 1992 Roermond earthquake, the Netherlands, and some of its aftershocks recorded at the stations of the Geological Survey of Northrhine-Westphalia – Geol. Mijnbouw, this issue

Plenefish, T. & K.-P. Bonjer 1994 The stress tensor in the Rhine Graben area derived from earthquake focal mechanisms (extended abstract) – Geol. Mijnbouw, this issue

Prinz, D., D. Hollnack & J. Wohlenberg 1994. The seismic activity near Aachen following the Roermond earthquake of April 13th, 1993 – Geol. Mijnbouw, this issue

Richter, C.F. 1935 An instrumental Earthquake Magnitude Scale – Bull. Seism. Soc. Am. 25: 1–32

Rosenhauer, W. & L. Ahorner 1994 Seismic hazard assessment for the Lower Rhine Embayment before and after the 1992 Roermond earthquake – Geol. Mijnbouw, this issue

Scherbaum, F. 1994 Modelling the Roermond earthquake of April 13, 1992 by stochastic stimulation of its high frequency strong motion – Geophys. J. Int. 119: 31–43

Van den Berg, M.W. 1994 Neotectonics of the Roer Valley rift system. Style and rate of crustal deformation inferred from syntectonic sedimentation – Geol. Mijnbouw, this issue

Van den Berg, M.W., W. Groenewoud, G.K. Lorenz, P.J. Lubbers, D.J. Brus & S.B. Kroonenberg 1994 Patterns and velocities of recent crustal movements in the Dutch part of the Roer Valley rift system – Geol. Mijnbouw, this issue

Ziegler, P.A. 1992 European Cenozoic rift system – Tectonophysics 208: 91–111

Ziegler, P.A. 1994 Cenozoic rift system of western and central Europe: An overview – Geol. Mijnbouw, this issue